Catena 202 (2021) 105282

Contents lists available at ScienceDirect

Catena

journal homepage: www.elsevier.com/locate/catena

Atterberg limits fail in recognizing fragipan horizons

S. Stanchi *, S. Negri, M.E. D'Amico, E. Raimondo, E. Bonifacio

University of Torino, Department of Agricultural, Forest and Food Sciences, Largo Braccini 2, 10095 Grugliasco, Italy

ARTICLE INFO

Keywords:
Fragic properties
Liquid limit
Plastic limit
Plastic index

ABSTRACT

Fragipan is a subsurface soil horizon characterized by high bulk density, coupled with an abundance of fine, blind pores. We hypothesized that this distinctive porosity pattern could affect the Atterberg limits, with significant deviations from those of otherwise comparable soil horizons. Additionally, longer pre-wetting times might be needed to determine the liquid and plastic limits in fragipan, due to restrictions in water movements. Based on these hypotheses, our research focused on (1) assessing the most suitable fragipan-specific sample preparation time for liquid and plastic limit determination; (2) evaluating if the Atterberg limits reflect the presence of fragic properties; (3) exploring the relationships between Atterberg limits and other relevant soil properties through Artificial Neural Networks. Fragipan horizons (F) had a slightly higher liquid limit, much higher bulk density, and specific surface area than nonfragipan (NF). The plastic limit was however comparable for F and NF. Thus, fragipans had a larger interval of plasticity, which is in contrast with slaking tests and well-known field evidence. Despite the expected differences between F and NF, three hours' pre-wetting was enough for all samples. This might be due to the size fraction used in the analysis, more sensitive to collapse upon water saturation than bigger clods. Atterberg limits did not help in discriminating F from NF, despite the relevant differences in other soil physical properties. Neural Networks showed that the transition from the plastic to the liquid state was mainly driven by texture and specific surface area, while the plasticity interval was mainly affected by the bulk density. These results provided further insights into the mechanical properties of fragipan horizons.

1. Introduction

Fragipan is a subsurface genetic horizon (Bx) described both in USDA and WRB soil classification systems (Soil Survey Staff, 2014; IUSS Working Group, 2015). It ischaracterized in the field by hardness, a blocky polygonal pattern (Smalley et al., 2016), and pronounced slaking upon wetting (Bockheim and Hartemink, 2013). Fragic properties can develop on a variety of parent materials, but they are often encountered on loess-derived soils. Examples can be found in the USA (Bockheim and Hartemink, 2013; Sun et al., 2018), in New Zealand (Yates et al., 2018; Vogeler et al., 2019), Poland (Szymanski et al., 2011), and in NW Italy (e.g. Negri et al., 2021).

Franzmeier et al. (1989) published a check-list of the characteristics of fragipan developed on loess, that can help field identification: acid silty and loamy deposits; limited slope; preferably forest vegetation; moist climate; long pedogenesis. The genesis and occurrence of fragipan on loess is still a subject of investigation, and no unique conclusion has been reached. Among the various hypotheses, Bryant's (1989) hydroconsolidation has received attention as it linked the behavior of fragipan and loess deposits, explaining the fragic properties of soils with physical processes that typically occur on loess and other unconsolidated deposits. Hydroconsolidation (Assallay et al., 1998; Rogers et al., 1994; Bryant, 1989) is indeed a widespread phenomenon occurring in loess soils, well known in engineering and geotechnics. When loess soils are loaded and wetted, they lose consistency and tend to self-collapse, just as fragipan does. Fragipan brittleness in the wet state, coupled with hardness when dry, narrows the range of functions and ecosystem services exerted by soils and impacts hydropedological and mechanical behavior (e.g. Franzmeier et al., 1989; Drohan et al., 2020). Brooks et al. (2012) remarked that fragipans have low drainable porosity, i.e. a low volume of water that can freely drain into the water table, with effects on subsurface lateral flow and surface runoff. This may result in water-saturated areas in the toe slope position or correspondence with shallower restricting layers, as documented by Wilson et al. (2010) in a catchment characterized by the extensive presence of fragipan. Also Gburek et al. (2006) underlined the relevance of fragipan for runoff generation and the overall hydrologic performance of the watershed.

The fragipan collapse upon wetting causes failures of buildings and

* Corresponding author.

https://doi.org/10.1016/j.catena.2021.105282
Received 27 November 2020; Received in revised form 3 February 2021; Accepted 27 February 2021
Available online 21 March 2021

infrastructures (e.g. Smalley et al., 2016), while prolonged dry periods result in a hard, brittle pan that limits the crop growth (Duiker, 2020) and makes trees more susceptible to uprooting in case of strong winds (Frost, 1981). We hypothesized that soil engineering properties such as the Atterberg liquid and plastic limits (ASTMD, 2010) might be suitable for the evaluation of the risks posed by fragipan presence in the soil, as they quantify the physical behavior of unconsolidated materials when exposed to water. In general, as thoroughly described in Wagner (2013), the soil water content largely affects the mechanical behavior in remolded soil samples. High liquid limit (LL) values point to high compressibility and great shrinkage/swelling potential. The difference between LL and plastic limit (PL), defined as the plastic index (PI), quantifies the range of plastic behavior in soils, i.e. the interval of water content in which the sample can deform without significantly losing strength. PI values exceeding 40 are typical of very plastic behavior, while values below 7 indicate non-plastic soils (Sovers, 1979). In the case of low PI values, even small variations in soil moisture can produce significant changes in consistency, together with low compressibility in soils.

Based on these considerations, fragipan is expected to show specific Atterberg limits, when compared to other soil horizons. To our knowledge, though, no general conclusions on the relationship between plastic properties and the presence of fragipan horizons have been drawn, nor clear differences between fragipan and other horizons types have been elucidated. Also the mechanisms at the base of the mechanical behavior suggest specificity in fragipans. Our previous research (e.g. Stanchi et al., 2017) detailed the main phases of water-soil particles interactions for increasing moisture contents in forest soils. The plastic limit is reached when soil shifts from the semi-solid to the plastic state, a condition met when water fills soil pores, excluding air. The well-known low porosity of fragipan (e.g. Bockheim and Hartemink, 2013), which is visible also in disturbed <2 mm samples (Falsone and Bonifacio, 2009), could underly a lower PL. The amount of water incorporated in the soil sample before it starts to flow freely (i.e. before liquefaction), in fact, can vary considerably depending on the clay content, as it is related to the amounts of water that can be absorbed by soil components before complete colloidal dispersion (Stanchi et al., 2017). Sand and silt-dominated textures usually show poor or no plasticity (i.e. low PI) due to the physical and surface properties of the particles. Therefore, plastic behavior should be expected from clay-rich samples, being they fragipan or not, if the contents of organic matter and mineralogical composition are similar.

The standard method for Atterberg limits determination might not be fully suitable for the characterization of fragipan horizons, that show blind and vesicular small pores, where water penetration may occur with difficulty (e.g. Ribeiro et al., 2015). In such methods in use for the determination of LL and PL, the < 0.425 mm soil fraction is pre-wetted with an amount of water exceeding LL, then the falling cone penetration (mm) is measured for decreasing moisture contents, as a combined effect of evaporation and sample remolding. The method suggests a settling of the wet sample varying up to 24 h according to the clay content before performing the fall tests (ASTMD, 2010; SISS, 1997). No further or clearer indication is given on this matter.

Even when only loess-derived fragipans are considered, the topic is developed more from an engineering perspective, thus clear links between Atterberg limits and genetic horizons are lacking, and the presence of fragipan is not always clearly mentioned. Additionally, geotechnical properties of loess and fragipan (LL, PL, PI) may vary widely (e.g. Delage et al., 2005; Yates et al., 2018; Assallay et al., 1996) depending on the general soil properties such as texture.

Given the complexity of the soil properties that can affect soil structure and consistency, partly derived from the loess parent material and partly affected by the presence of fragipan itself, we explored the ANNs (Artificial Neural Networks) technique to gain insight into the soil properties and their relationships. ANNs proved to be a powerful and flexible tool to explore complex processes, and require minimal demand and model assumptions. They can be successfully used for data mining and/or predictive purposes, to model complex relationships between input (independent) variables and output (dependent) variables, identifying non-linear structures (e.g. Mahana, 2017). Many applications in soil science already exist, where ANNs demonstrated better accuracy than regression techniques (see e.g. Honorato Fernandes et al., 2020, and cited literature). For example, they have been extensively applied to investigate the soil hydraulic properties (Mojid et al., 2019) and soil degradation processes (e.g. Gholami et al., 2021), and thus could be potentially interesting for our purposes. Thus, we combined more classical methods (e.g. ANOVA and correlations) with ANNs.

We hypothesized that the typical porosity of loess-derived fragipan horizons could deeply affect their engineering properties, deviating from that of otherwise comparable soil horizons. Therefore, this research aimed at (1) assessing the most suitable fragipan-specific sample preparation time for LL and PL determination, considering its distinctive properties; (2) assessing a range of variation of LL, PL, PI in fragipan, and evaluating if the Atterberg limits closely mirror the presence of fragic properties; (3) exploring the relationships between LL, PL, and PI and other relevant soil properties.

2. Materials and methods

The study area is located in NW Italy (Fig. 1), where soils developed on fluvioglacial terraces dating back to Middle-Upper Pleistocene, i.e. around 700000 to 130000 years BP (Forno et al., 2007). The lithology of the fluvial and fluvioglacial substrate in the Lanzo alluvial fan is mainly ultramafic (Raimondo et al., 2019). Querco-Carpinetum is the native vegetation type, dominated by species like oak (*Quercus robur* L.) and hornbeam (*Carpinus betulus* L.). Crops or hay meadows mostly took over the original forest cover.

Soils have been classified as Typic Fragiudalfs (Soil Survey Staff, 2014) or Fragic Luvisols (Siltic, Profondic) (IUSS Working Group, 2015) with a mesic temperature regime. In the area, fragipan horizons, appearing at a depth of 60–70 cm from the ground surface, display very low organic carbon contents and high bulk densities (Falsone and Bonifacio, 2006).

Five soil profiles were described in the field and sampled. The soil horizons used for our study are listed in Table 1, together with profile and site information. Half of the samples (total n = 30) were fragipan horizons. Bulk density (BD) was measured by the core method (Blake and Hartge, 1986).

Na–dithionite–citrate bicarbonate–extractable Fe (Fe_{DCB}) was quantified (Mehra and Jackson, 1960).

Air-dried samples were sieved at 0.425 mm for LL and PL determination according to British Standards Protocol (ASTMD, 2010). Two sample pre-wetting times were applied, 3 and 24 h. LL was determined by the cone penetrometer method and PL was measured with the thread-rolling method. Specific surface area (SSA) was estimated on the same fraction by the methylene blue adsorption method (ASTM, 1984). Particle-size distribution (PSD) was determined by the pipette method (Gee and Bauder, 1986) after Na-hexametaphosphate dispersion. No cements, organic or iron-related, were removed. PSD data were then used to compute the fragmentation fractal dimension D_f, using the mass-based approach described in Tyler and Wheatcraft (1992) and then applied e.g. by Stanchi et al. (2008), to investigate the distributions of primary particles and aggregates in different soil types and horizons. D_f ranges from 2 to 3: values tending to 3 indicate more pronounced fragmentation, i.e. a distribution dominated by finer sizes, while D_f close to 2 indicates an abundance of coarser sizes. It was adopted to better compare PSDs of different horizon types and to identify possible trends with soil depth/horizon types.

All statistical analyses were conducted with SPSS ver. 25. A paired-sampled *t*-test was applied to compare results from different preparation times (3 vs. 24 h), One-way ANOVA was used to compare fragipan vs. non-fragipan horizons. We then run ANNs (multilayer perception,

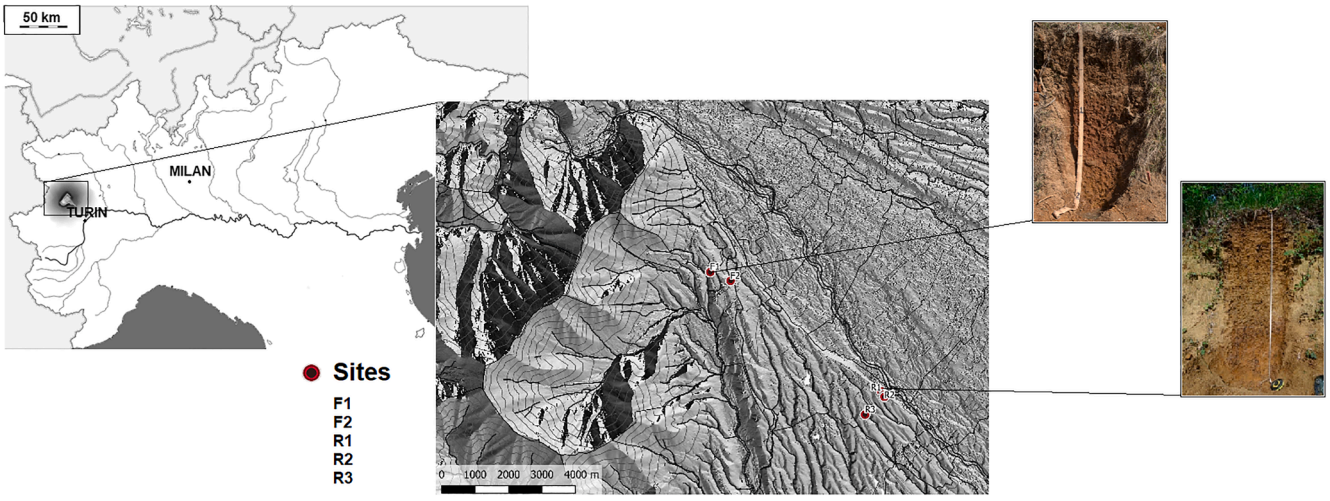

Fig. 1. Study area location.

Table 1
Profile location and horizons used for the present research.

Profile location	ID	Latitude	Longitude	Horizons considered in the present study
Fiano	F1	45° 13′ 35.544″N	7° 30′ 56.31″ E	Bw1;Bw2; 2Bc; 2Btc; 2Bt1; 2Bt2
Fiano	F2	45° 13′ 31.03″ N	7° 31′ 29.83″ E	A/B; Bg; 2Btx1; 2Btx2; 3Btx; 4Bx
Robassomero	R1	45° 11′ 21.83″ N	7° 34′ 27.51″ E	Bw; 2Bx1; 2Bx2; 2Bx3; 2Bvt; 4Btx
Robassomero	R2	45° 11′ 28.36″ N	7° 35′ 15.78″ E	Eg; 2Bv; 2Bx; 2Btx; 3Btx; 3Bv
Robassomero	R3	45° 11′ 25.43″ N	7° 35′ 12.71″ E	Bw ; 2Btx; 2E/Bx; 2Btx; 3Btxv ; 3Bx

batch training) to spot information hidden in the dataset and to explore the properties that drive typical fragipan behavior. The method is briefly summarized in Fig. 2. The model is a function of predictors (i.e. inputs or independent variables) that minimize the prediction error of target variables (i.e. outputs). An input layer (i.e. the group of predictive variables) is connected with one or more nodes (H1, H2, etc.) that represent the "hidden layer". The value of each hidden unit is some function of the input layer, conceptually comparable to a regression, whose form depends on the network properties and user settings. The resulting variable (output layer) is a response of the functions connecting the nodes with the output. Each input variable appears in the functions with a specific weight indicated by the line thickness. Bias is quantified, too, and the goodness of the prediction can be assessed by comparing predicted vs. measured values of the target variable.

3. Results

The main soil properties for F samples (n = 15), NF samples (n = 15), and the whole group of soil samples (n = 30) are displayed in Table 2. The textures were loam, clay-loam, silt-loam, silty-clay-loam, and clay, with poor coarse sand content (average 4.3%, n = 30). Fragipan horizons were mainly clay-loams and loams, with less coarse sand than NF

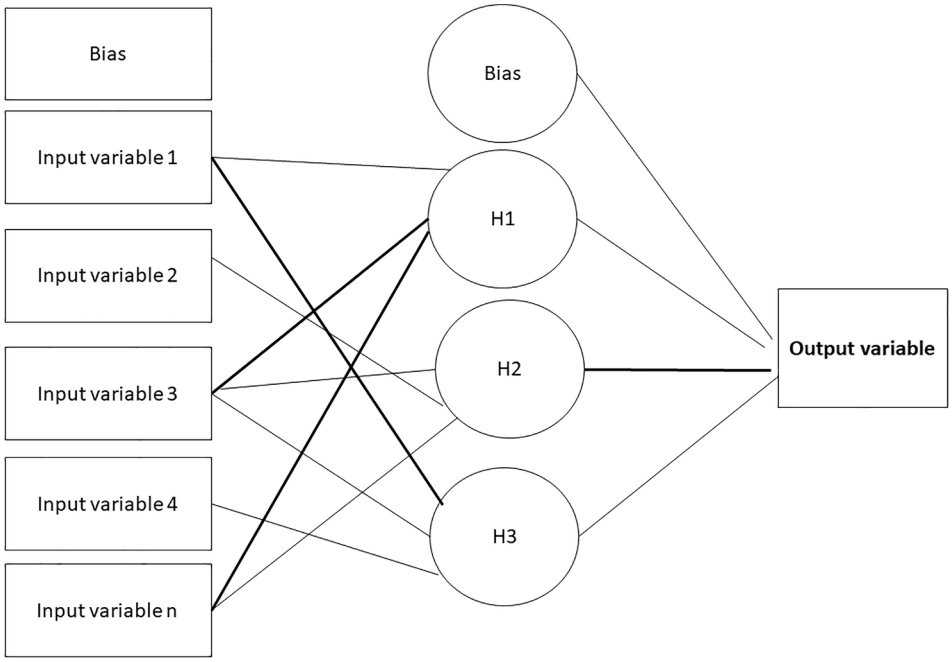

Fig. 2. Schematic representation of ANNs (Artificial Neural Networks).

Table 2
Soil properties for F (fragipan) and NF (non-fragipan) soil samples. The standard deviation is in brackets. Low case letters indicate differences between F and NF. * indicates $p < 0.05$, ** indicates $p < 0.01$.

Fragipan	Coarse sand (%)	Fine sand (%)	Coarse silt (%)	Fine silt (%)	Clay (%)	D_f (–)	LL_{3h}(%) LL_{24h}(%)	PL_{3h}(%) PL_{24h}(%)	PI (%)	SSA (m^2 g^{-1})	Fe_{DCB} (g kg^{-1})	PI/LL_{3h} PI/LL_{3h}	BD (g cm^{-3})
NF (n = 15)	5.3a* (2.91)	23.8 (6.27)	19.6 (4.90)	27.3(4.36)	23.9 (7.17)	2.783 (0.041)	36(4.3) b* 36(4.5) b*	29(3.7) 29(3.5)	7(2.1) b* 7(2.0) b*	25.76b** (11.47)	30.72 (14.57)	0.19 (0.050) 0.22 (0.056)	1.45b* (0.17)
F (n = 15)	3.3b* (1.69)	23.8 (10.4)	20.2 (3.05)	25.1 (2.22)	27.6 (6.53)	2.804 (0.036)	39(3.5)a 39(3.9)a	31(2.8) 31(3.0)	9(2.8) a 8(2.6) a	40.23 (7.93)a**	26.44 (7.66)	0.18 (0.044) 0.21 (0.054)	1.59a* (0.15)
TOT (n = 30)	4.3 (2.53)	23.8 (5.94)	19.9 (4.03)	26.2 (3.60)	26.2 (3.60)	2.793 (0.039)	38(4.1) 38(4.4)	30(3.1) 30(3.3)	8(2.7) 7(2.5)	32.99 (12.17)	28.58 (11.64)	0.20 (0.054) 0.20 (0.052)	1.52 (0.15)

(5.3% vs 3.3%, $p < 0.05$). The silt contents were rather homogeneous (>45%); the average clay contents always > 22%. The fractal dimension D_f did not underline any differences between sample types and was on the average 2.793 (n = 30). As visible in Table 2, the most relevant differences were observed in SSA, which was much higher in fragipans (average 40.23 m^2 g^{-1} vs. 25.76 m^2 g^{-1}, $p < 0.01$), and BD (again, higher in fragipans, with average value 1.59 g cm^{-3} vs. 1.45, $p < 0.05$). The Fe_{DCB} contents were instead comparable in the subsets, with a global average of 28.58 g kg^{-1} but a large dispersion around the mean, especially for NF samples.

LL, regardless of the pre-wetting time, was higher for F samples (39%, $p < 0.01$) than for NF samples (36%). PI was significantly higher for F ($p < 0.05$), although the difference between the two groups was only 2% (Table 2). All samples fell close to the lower PI threshold (7%) of medium plasticity according to the classification of Sovers (1979).

LL, PL, and PI values for the 2 pre-wetting times (3 vs. 24 h) were compared using a paired-samples *t*-test which gave $p = 0.354$, $p = 0.815$, and $p = 0.566$, respectively, i.e. equal values of Atterbeg limits and plastic index independent of the pre-wetting time used in the test (n = 30). To exclude the presence of different behaviors according to the type of horizons, we split the whole dataset into the two groups (n = 15 each) and re-run the *t*-test, obtaining comparable results: the significance was $p = 0.366$, $p = 0.682$, and $p = 0.709$, for LL, PL, and PI respectively for NF samples, and $p = 0.709$, $p = 0.907$, and $p = 0.676$ for F samples. Fig. 3 shows the plots of LL and PL depending on the duration of pre-wetting time. Considering F vs. NF samples, no systematic deviation pattern could be visually observed from the 1:1 line, and no clear pattern in the distribution of samples above or below the line was visible as well. As no significant difference was observed between pre-wetting time before LL and PL determination, we only considered LL_{3h} and PL_{3h} for further statistics.

In engineering, the plastic properties of soil samples are usually represented in the Casagrande chart (Casagrande, 1948), i.e. a plot of PI vs. LL, where threshold values of the two variables identify different regions of geotechnical behavior and consistency. The chart, as for the USDA soil textural triangle in soil science and agronomy, is a widely used soil classification system in engineering (Moreno-Maroto and Alonzo-Azcarate, 2018). In the Casagrande chart (Fig. 4), all samples were classified as organic or inorganic silts with medium compressibility and showed (PI/LL) < 0.33, i.e. they were silts with low plasticity, according to the modified Casagrande Chart suggested by Moreno-Maroto and Alonzo-Azcarate (2018).

LL and PL were significantly correlated in the whole dataset ($r = 0.779$, $p < 0.01$, n = 30), and they also showed significant, although rather weak, correlation with the clay content ($r = 0.589$, $r = 0.584$, $p < 0.01$, n = 30). LL was correlated with SSA ($p = 0.779$, $p < 0.01$, n = 30).

Considering the two groups separately (F vs. NF), contrasting trends in correlation coefficients were observed (Table 3). The strong correlation between LL and PL, observed in the whole dataset, dropped when considering the subsets separately ($r = 0.579$, $p < 0.05$ in F; $r = 0.832$, $p < 0.001$ in NF). PI was correlated with LL only in fragipans ($r = 0.675$, $p < 0.01$). SSA was strongly correlated with PI in the fragipan subset alone, ($r = 0.870$, $p < 0.01$). The Fe content resulted tightly linked with the Atterberg limits in both the subsets, even if the relationship was particularly evident with LL in the NF subset ($r = 0.764$, $p < 0.01$). Clay was strongly related to LL in the case of F but, in the same subset, not

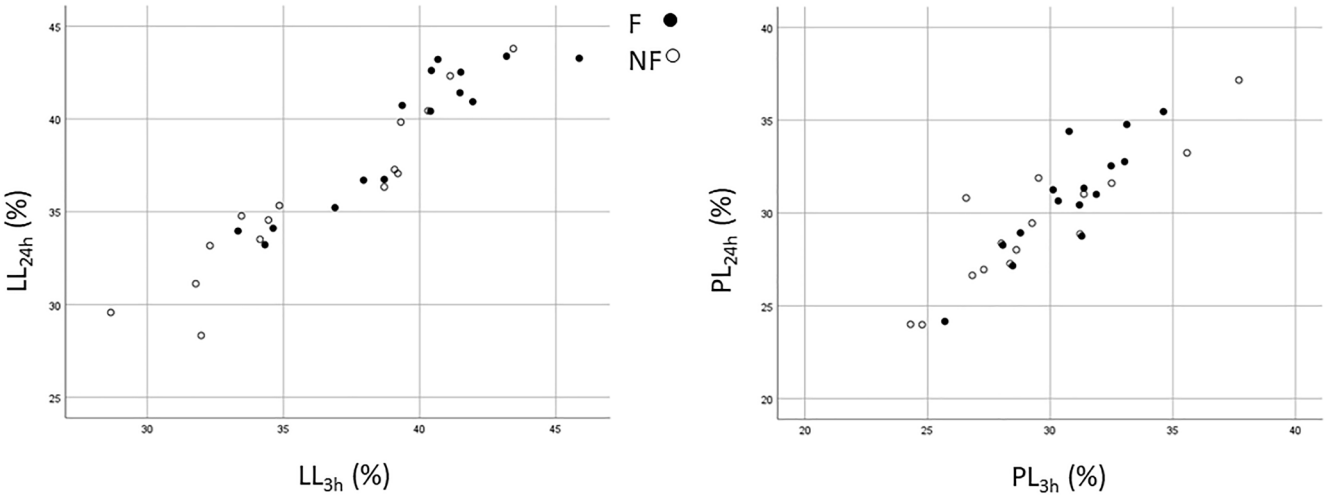

Fig. 3. Liquid and plastic limits determined for 3 and 24 h pre-wetting times.

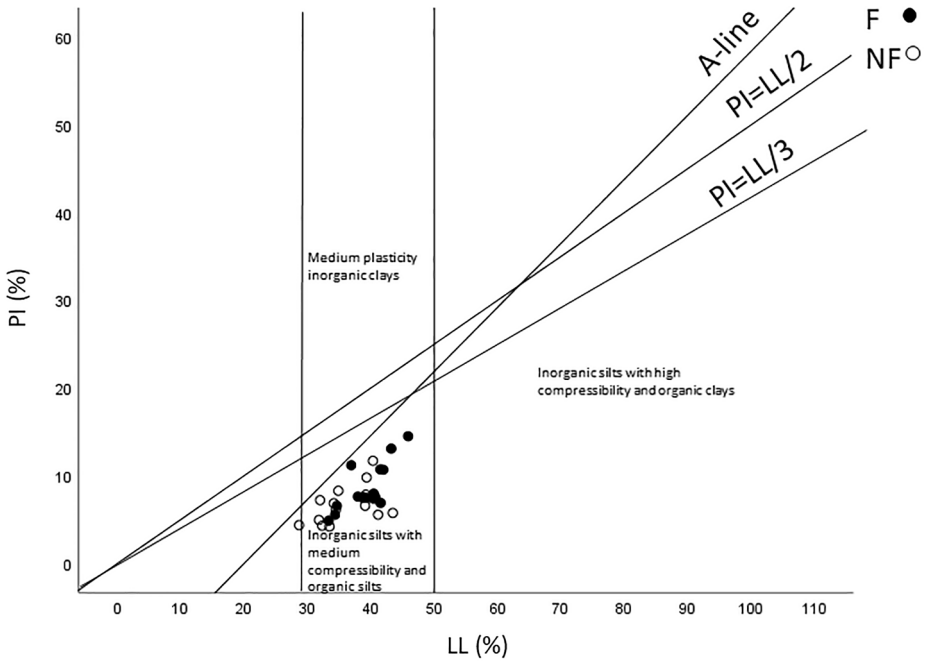

Fig. 4. Casagrande chart for the studied samples, as modified by Moreno-Maroto and Alonzo-Azcarate (2018).

Table 3
Correlations between soil properties for F and NF samples. *indicates $p < 0.05$, ** indicates $p < 0.01$. In bold, significant correlations with r coefficients > 0.5.

NF samples (n = 15)	LL(%)	PL(%)	PI (%)	SSA ($m^2\ g^{-1}$)	Fe_{DCB} ($g\ kg^{-1}$)	Clay(%)	BD ($g\ cm^{-3}$)	PI/LL
LL_{3h}(%)	–	**0.832****	0.482*	**0.673****	**0.764****	**0.757****	0.214	0.164
PL_{3h}(%)		–	0.079	**0.572***	**0.575***	**0.518***	0.404	−0.264
PI (%)			–	0.401	0.325	0.307	−0.154	−0.354
SSA ($m^2\ g^{-1}$)				–	**0.564***	**0.519****	0.392	0.129
Fe_{DCB} ($g\ kg^{-1}$)					–	**0.882****	0.379	0.107
Clay						–	0.379	0.376
F samples (n = 15)								
LL(%)	–	**0.579***	**0.675****	**0.552***	**0.611***	**0.933****	**−0.574***	**0.525****
PL(%)		–	0.021	0.127	**0.668****	0.492*	−0.101	−0.175
PI (%)			–	**0.870****	0.089	**0.752***	**−0.623***	**0.954****
SSA ($m^2\ g^{-1}$)				–	0.234	**0.617****	−0.470**	**0.854****
Fe_{DCB} ($g\ kg^{-1}$)					–	**0.525****	−0.007	−0.036
Clay (%)						–	**−0.584***	**0.597****

with PL. Correlations between bulk density and other soil properties were visible only in fragipan horizons (particularly with PI, $r = -0.623$, $p < 0.05$). PI/LL showed consistent correlation coefficients with SSA for fragipans (always $r > 0.85$, $p < 0.01$), while poorer relationships were observed with LL and clay content (Table 3).

ANNs (Fig. 5) helped to quantify the influence of soil properties (BD, SSA, Fe_{DCB}, D_f) on LL, PL, and PI as target variables in the studied soils. In the prediction of LL (Fig. 5) one hidden layer (hyperbolic tangent activation function, 2 units) was identified, and the variable was predicted by D_f, SSA, Fe_{DCB}, BD with importance 0.381, 0.362, 0.181, and 0.067, respectively. The R^2 of LL predicted vs. measured was 0.74. PL prediction was not satisfactory, as the R^2 of PL predicted vs. measured was 0.44 (thus, the ANNs structure is not shown). PI was instead successfully predicted ($R^2 = 0.81$). The ANN structure (Fig. 5) included

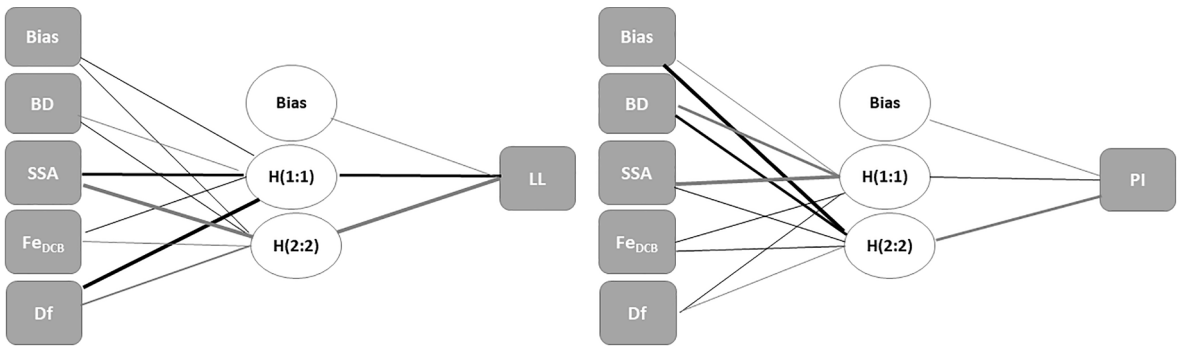

Fig. 5. Results of the Artificial Neural Network application for LL and PI estimates.

again one hidden layer with two units and a hyperbolic tangent activation function. The importance of the variables was: 0.363 for BD, 0.288 for SSA, 0.204 for D_f, and 0.145 for Fe_{DCB}. Changing the order of input variables did not affect significantly the ANN outputs.

4. Discussion

Fragipan soil horizons did not display significant differences from the others in terms of textures, that were in general comparable to those reported in the literature (Bockheim and Hartemink, 2013; Ciolkosz and Waltman, 2000). Fragipan horizons (Btx, Bx, Btxv, etc.) had similar particle-size distribution as NF (Btc, Bc, A/B, Bg, Bw, Eg) and, in particular, they showed comparable clay contents. Therefore, D_f, as a synthetic index for aggregate-size distribution, did not evidence any significant differences. Being D_f computed from the cumulative mass-size distribution after Na-hexametaphosphate dispersion, we can conclude that the stability of the clay-containing aggregates towards chemical dispersants was similar for all soil horizons. As the linkages among particles hypothesized by Smalley et al. (2016) in fragipan do not involve any chemical bond, the similar sensitivity of F and NF towards Na-hexametaphosphate is probably related to the presence of comparable amounts of pedogenic Fe oxides acting as cementing agents (Table 2).

The higher bulk density of F samples, ranging from 1.45 to 1.75 g cm^{-3}, was comparable with data from Lindbo et al. (1994), who reported a range of 1.45–1.78 g cm^{-3} for fragipan horizons of Glossic Fragiudalfs in the US, and with Matocha et al. (2018) who studied Typic Fragiauldalfs forming on loess in South-Eastern USA (range 1.62–1.78 g cm^{-3}). Thus, F samples had lower total porosity, as expected.

A comparison of the results obtained with the two selected sample wetting times (3 vs. 24 h) did not evidence any differences in Atterberg limits determination. Therefore, despite our initial hypothesis that the typical porosity pattern of fragipan might be able to affect water infiltration and retention, a pre-wetting time of 3 h seems to suffice for the analysis. We can now hypothesize two reasons to explain this behavior. First, the samples used for LL and PL determination are not undisturbed. They are indeed a subfraction of the fine earth obtained by sieving (< 0.425 mm), as required by the standard method adopted to determine Atterberg limits (ASTMD, 2010). These small aggregates are completely exposed to water infiltration into pores during wetting, while in the case of bigger clods only the external surface would be exposed, requiring a longer time for water to fill the aggregate porosity, as commonly observed in the field. Secondly, differences might occur, but in a very short time range, i.e. much less than 3 h. However, the experiment helped in the optimization of the test. Thus, longer and time-consuming protocols can now-on be avoided.

As stated in the introduction, the Atterberg limit values reported in the literature for loess-derived fragipan horizons are quite variable, probably due to the heterogeneity of clay contents and the adopted sampling strategies, often carried out at fixed depths rather than by single genetic horizons. For example, Yates et al. (2018) and cited literature reported the geotechnical properties of soil horizons defined as Bx or Cx, with clay contents comparable with our samples (i.e. 18–32% vs. 14–40% in our work). They found LL values in the range of 24–30%; PL and PI in ranges of 16–19% and 6–11%, respectively. Our samples displayed LL values of 33–46%, PL in the range of 26–34%, and PI spanning from 5 to 14%. Fragipan samples showed slightly, but significantly, higher LL than non-fragipan (Table 2). This was not expected, considering the similar clay contents and the good correlation between clay and LL typically found in the literature for a wide variety of soils (e.g Moradi and Ebrahimi, 2013; Ural, 2015), as well as in both subsets of this study (Table 3). As the effect of organic matter can be excluded, considered the very low amounts found in all horizons (Falsone and Bonifacio, 2006), the difference may therefore depend on the much higher SSA found in fragipans, resulting in a higher water absorption capacity of these horizons. The higher SSA of fragipan horizons, despite the comparable amounts of clay, points to a typical aggregation pattern in fragipans, or a different mineralogical composition of the clay fraction. These fragipans were slightly enriched in kaolinites (ca. 8–9% more), and poorer in chlorite-vermiculite mixed layers (ca. 9–10%) with respect to non-fragipans (Raimondo et al., 2019). Kaolinites have a low surface area (30–55 $m^2\ g^{-1}$, Khawmee et al., 2013), which is likely to be only slightly smaller than that of the mixed-layer mineral when measured by the methylene blue test. The internal surface area would indeed not be accessible when occupied by Al-polymers (Malla, 2002), thus these small mineralogical differences are not likely to induce a doubled SSA in F vs. NF horizons. Furthermore, the activity index A, computed as PI/clay (Table 2) was comparable for F and NF, and typical of "inactive clays" (A < 0.75, according to Kaliakin, 2017) such as kaolinite. A different aggregation pattern in fragipan is expected, and the higher microporosity, linked to the open packing of the clay fraction (Falsone and Bonifacio, 2006) may indeed explain the higher SSA. The relationship between clay and microporosity in the F samples is further confirmed by the negative correlation coefficient between BD and clay, which is visible only in this type of soil horizons.

Being the PL similar in F and NF horizons, the plasticity interval was higher in fragipans, even if both F and NF samples stood at the lower threshold of moderate plasticity according to Sovers (1979). However, more recently, Moreno-Maroto and Alonzo-Azcarate (2018) proposed that the soil should be considered non-plastic when PI is less than LL/3, regardless of the amounts of clay. In our study area, this is true for all samples independent of the horizon type. Again, only in F samples, PI showed a strong relationship with SSA, as expected if the differences in the interval of plasticity are linked to the variability of LL.

The correlation between LL and PL is commonly reported in the literature for a wide range of soils with heterogeneous chemical and physical properties (as texture, clay, and organic matter content). However, this relationship appeared to be much less pronounced in fragipan (Table 3).

Based on the obtained Atterberg limits and indexes, the F samples could absorb more water before complete liquefaction, keeping a plastic behavior for a wider range of water content. This seems to be in contrast to the well-known brittleness of fragipan upon wetting. Before performing the geotechnical test, we checked on small amounts of the < 0.425 mm size fraction if slaking would occur, and we could visually confirm the phenomenon. However, as remarked by Lal (2006), PI indicates the sample sensitivity towards changes in water content but does not fully explain soil mechanical stability. In our dataset, the Atterberg limits (particularly PL) and PI were not able to capture the typical behavior of fragipan, which could instead clearly be observed in the lab and the field.

The negative correlation between BD and LL (Table 3) observed only for F samples suggests that, when the density increases, a lower amount of water is needed to reach the liquid state, i.e. to obtain complete clay dispersion. This points to a greater vulnerability towards aggregate failure upon wetting, in case of horizons with more pronounced fragic properties (ie. higher BD, lower porosity), that would require less water to lose their strength till complete collapse. This is not true in NF samples, that are not affected by slaking.

Artificial Neural Networks underlined the relative importance of the soil properties that are determining the Atterberg limits in the soil dataset. However, only LL and PI could be successfully predicted, as visible in Fig. 5. In both cases, the importance of finer size classes (i.e. D_f), their arrangement (SSA), and the density of the sample were the retained variables. Their importance varied, with D_f and SSA being the most influential variables in LL prediction, and BD weighing more than all other variables in PI. In literature, the importance of clay (thus D_f) has been widely described, but also a relationship between SSA and LL has been observed in soil (e.g. Arnepalli et al., 2008). This seems once again to confirm the importance of clay and of the extent of surfaces available for dispersion in water when dealing with liquefaction, while the total amounts of filled pores might have some importance in PI

indirectly, affecting the amounts of water retained at PL. The ANNs, therefore, point towards a mechanical behavior in fragipans which is driven by the same determinant factors that operate in other soil horizons.

All these findings suggest that despite fragipans show typical physical properties, the Atterberg limits are not suitable enough to capture the fragipan specific features in the studied soils.

5. Conclusions

This research investigated the mechanical behavior of fragipans. An improvement of the existing protocols for LL and PL determination has been proposed and the relationships existing between Atterberg limits and other relevant soil properties have been investigated. No difference in LL, PL, and PI emerged by comparing results from 3 h vs. 24 h sample pre-wetting times. Hence, the shortest of the two time spans proved to be suitable for the determination of Atterberg limits even for F samples, despite their high microporosity and peculiar pore pattern. We recommend therefore the adoption of this wetting time for future lab tests to avoid time-consuming procedures.

Fragipan horizons had significantly, although slightly, higher LL and PI, much higher bulk density and SSA than non-fragipan horizons. However, the Atterberg limits alone failed in capturing the peculiarity of fragipans. This might be due to the size fraction required for the Atterberg limits determination standards, combined with the fact that the method is destructive and cannot fully mirror the mechanisms occurring at larger scales. Atterberg limits, and particularly PL, alone did not help in discriminating F from NF as successfully as visual recognition and slaking tests. In fact, F and NF samples, despite the strong differences observable in the field and macro-aggregate scale, showed only very small differences in two of the considered geotechnical indexes (LL, PI), while strong differences were visible in other properties.

In the study dataset, the transition from the plastic to the liquid state (i.e. LL, complete clay dispersion) was mainly governed by the abundance of fine aggregates and SSA, while the property that mostly affected the plasticity interval (PI) was BD, that is strictly related with the total porosity. Further insights on the mechanical properties of fragipan horizons were therefore provided. These findings could come useful in the study of fragipan-affected soils, given their wide distribution in temperate climates and the relevant limitations they pose due to their distinctive physical properties, and once more underline the importance of field observation and slaking testing in fragipan recognition.

Declaration of Competing Interest

The authors declare that they have no known competing financial interests or personal relationships that could have appeared to influence the work reported in this paper.

References

Arnepalli, D.N., Shanthakumar, S., Hanumantha, R.B., Singh, D.N., 2008. Comparison of methods for determining specific-surface area of fine-grained soils. Geotech. Geol. Eng. 26, 121–132.

Assallay, A.M., Rogers, C.D.F., Smalley, I.J., 1996. Engineering properties of loess in Libya. J. Arid Environ. 32, 373–386.

Assallay, A.M., Jefferson, I., Rogers, C.D.F., Smalley, I.J., 1998. Fragipan formation in loess soils: development of the Bryant hydroconsolidation hypothesis. Geoderma 83, 1–16.

ASTM, 1984. Standard Test Method for Methylene Blue Index of Clay. C 837-81 Section XV. 15.02.

ASTMD 4318–10e1, 2010. Standard Test Methods for Liquid Limit, Plastic Limit, and Plasticity Index of Soils. ASTM International, West Conshohocken, PA.

Blake G.R., Hartge K.H., 1986. Bulk density. In: Klute, A. (ed.) Methods of soil analysis. Part 1. 2nd ed. Agron. Monogr. 9. ASA and SSSA, Madison, WI, pp. 363–375.

Bockheim, J.G., Hartemink, A.E., 2013. Soils with fragipan in the USA. Catena 104, 232–242.

Brooks, E., Boll, J., McDaniel, P.A., 2012. Hydropedology in seasonally dry landscapes: the palouse region of the Pacific Northwest USA. In: Lin, H. (Ed.), Hydropedology. Elsevier, pp. 329–350.

Bryant R.B., 1989. Physical processes of fragipan formation. In: Smeck, N.E., Ciolkosz, E. J.Ž. (eds.), Fragipans: Their Occurrence, Classification and Genesis. Soil Sci. Soc. Am. Spec. Publ. 24, pp. 141–150.

Casagrande, A., 1948. Classification and identification of soils. ASCE Trans. 113, 901–991.

Ciolkosz, E.J., Waltman, W.J., 2000. Pennsylvania's Fragipans. Agronomy Series Number 147, Agronomy Department. The Pennsylvania State University, pp. 1–12.

Delage, P., Cui, Y.J., Antoine, P., 2005. Geotechnical problems with loess deposits in Northern France. Proceedings of International Conference on Problematic Soils, GEOPROB.

Drohan, P.J., Thompson, J.A., Lindbo, D.L., Beaudette, D.E., Dadio, S.D., 2020. Redefining the fragipan to improve field recognition and land use relevance. Soil Sci. Soc. Am. J. 84, 1055–1066.

Duiker, S.W., 2020. In-row subsoiling benefits maize yield on soil with a shallow fragipan. Crop, Forage Turfgrass Manage. https://doi.org/10.1002/cft2.20008.

Falsone, G., Bonifacio, E., 2006. Destabilization of aggregates in some typic Fragiudalfs. Soil Sci. 171, 272–281.

Falsone, G., Bonifacio, E., 2009. Pore-size distribution and particle arrangement in fragipan and non fragipans horizons. J. Plant Nutr. Soil Sci. 172, 696–703.

Forno, G.M., Gregorio, L., Vatteroni, R., 2007. La successione stratigrafica del settore destro del Conoide di Lanzo e il suo significato per l'utilizzo del territorio. Memorie Società Geologica Italiana 87, 237–247.

Franzmeier D.P., Norton L.D., Steinhardt G.C., 1989. Fragipan Formation in Loess of the Midwestern United States. In: Smeck, N.E., Ciolkosz, E.J. (wds.), Soil Sci. Soc. Am. Spec. Publ. 24, pp. 69–97.

Frost, L.W., 1981. Soil Survey of Columbia, McDuffie, and Warren Counties. Soil Conservation Service, University of Georgia (USA), Georgia, p. 130.

Gee, G.W., Bauder, J.W., 1986. Particle-size analysis. Methods of soil analysis: Part 1. 2nd Ed. A. Klute. Agronomy Monograph 9, 383–411.

Gburek, W.J., Needelmann, B.A., Srinivasan, M.S., 2006. Fragipan controls on runoff generation: Hydropedological implications at landscape and watershed scales. Geoderma 131, 330–344.

Gholami, H.S., Sahour, H., Amri, M.A.H., 2021. Soil erosion modeling using erosion pins and artificial neural networks. Catena 196. https://doi.org/10.1016/j.catena.2020.104902.

Honorato Fernandes, M.M., Prates, Coelho A., Flavio da Silva, M., Scabello, Bertonha R., Fernandes de Queiroz, R., Angeli Furlani, C.E., Fernandes, C., 2020. Estimation of soil penetration resistance with standardized moisture using modeling by artificial neural networks. Catena 189. https://doi.org/10.1016/j.catena.2020.104505.

Kaliakin, V.N. (Ed.). 2017. Soil Mechanics. Calculations, Principles, and Methods. Elsevier, 462 p.

Khawmee, K., Suddhiprakarn, A., Kheoruenromne, I., Singh, B., 2013. Surface charge properties of kaolinite from Thai soils. Geoderma 192, 120–131.

IUSS Working Group WRB. 2015. World Reference Base for Soil Resources 2014, update 2015. International soil classification system for naming soils and creating legends for soil maps. World Soil Resources Reports No. 106. FAO, Rome.

Lal, R. (Ed.), 2006. Encyclopedia of Soil Science, 2nd ed.. Taylor & Francis, New York.

Lindbo, D.L., Rhoton, F.E., Bigham, J.M., Jones, F.S., Smeck, N.E., Hudnall, W.H., Tyler, D.D., 1994. Bulk density and fragipan identification in loess soils of the lower mississippi river valley. Soil Sci. Soc. Am. J. 58, 884–891.

Mahana, J., 2017. Introduction to neural networks, advantages and applications. Data Sci. (2017) KDnuggetsTM News 17:n28, Jul 26.

Malla, P.B., 2002. Vermiculites, In Soil mineralogy with environmental applications. SSSA Book series no.7. Madison, WI. pp. 501–529.

Matocha, C.J., Karathanasis, T.D., Murdock, J.H.G., Goodman, J., Call, D., 2018. Influence of ryegrass on physico-chemical properties of a fragipan soil. Geoderma 317, 32–38.

Mehra, O.P., Jackson, M.L., 1960. Iron oxide removal from soils and clays by a dithionite-citrate system buffered with sodium bicarbonate. Clay. Clay Miner. In: Proc. 7th National Conference on Clays and Clay Minerals, Washington, DC, 1958, pp. 317–327.

Mojid, M.A., Hossain, A.B.M.Z., Ashraf, M.A., 2019. Artificial neural network model to predict transport parameters of reactive solutes from basic soil properties. Environ. Pollut. 255 https://doi.org/10.1016/j.envpol.2019.113355.

Moradi, S., Ebrahimi, E., 2013. Relationship between the percentage of clay with liquid limit, plastic limit and plastic index in four different soils texture class. Tech. J. Eng. Appl. Sci. 3, 692–702.

Moreno-Maroto, J.M., Alonzo-Azcárate, J., 2018. What is clay? A new definition of "clay" based on plasticity and its impact on the most widespread soil classification systems. Appl. Clay Sci. 161, 57–63.

Negri, S., Raimondo, E., D'Amico, M.E., Stanchi, S., Basile, A., Bonifacio, E., 2021. Loess-derived polygenetic soils of North-Western Italy: A deep characterization of particle size, shape and color to draw insights about the past. Catena 196. https://doi.org/10.1016/j.catena.2020.104892.

Raimondo, E., Falsone, G., D'Amico, M., Stanchi, S., Celi, L., Bonifacio, E., 2019. Characteristics of fragipan B horizons developed on different parent material in North-Western Italy. Arch. Agron. Soil Sci. 65, 308–321.

Ribeiro, Ramos M., Freitas, Melo V., Uhlmann, A., Dedecek, R.A., Ribas, Curcio G., 2015. Clay mineralogy and genesis of fragipan in soils from Southeast Brazil. Catena 135, 22–28.

Rogers, C.F.D., Dijkstra, T.A., Smalley, I.J., 1994. Hydroconsolidation and subsidence of loess: Studies from China, Russia, North America and Europe: In memory of Jan Sajgalik. Eng. Geol. 37, 83–113.

S.I.S.S., 1997. Metodi di analisi chimica del suolo, Franco Angeli, Milano, Italia.
Smalley, I.J., Bentley, S.P., Markovic, S.B., 2016. Loess and fragipans: Development of polygonal-crack-network structures in fragipan horizons in loess ground. Quat. Int. 399, 288–1233.
Soil Survey Staff, 2014. Keys to Soil Taxonomy, 12th ed. USDA-Natural Resources Conservation Service, Washington, DC.
Sovers, 1979. Introductory Soil Mechanics and Foundations: Geotechnical Engineering, 4th ed., Macmillan, New York.
Stanchi, S., Bonifacio, E., Zanini, E., 2008. Mass-size fractal dimension of primary and aggregated particles and soil profile development. Soil Sci. 173, 87–95.
Stanchi, S., Catoni, M., D'Amico, M.E., Falsone, G., Bonifacio, E., 2017. Liquid and plastic limits of clayey, organic C-rich soils: Role of organic matter and mineralogy. Catena 151, 238–1146.
Sun, Z.X., Jiang, Y.Y., Wang, Q.B., Owens, P.R., 2018. Fe-Mn nodules in a southern Indiana loess with a fragipan and their soil forming significance. Geoderma 313, 92–111.
Szymanski, W., Skiba, M., Skiba, S., 2011. Fragipan horizon degradation and bleached tongues formation in Albeluvisols of the Carpathian Foothills, Poland. Geoderma 167–168, 340–350.
Tyler, S.W., Wheatcraft, S.W., 1992. Fractal scaling of soil particle-size distributions: Analysis and limitations. Soil Sci. Soc. Am. J. 56, 362–369.
Ural, N., 2015. The relationship between geotechnical index properties and the pore-size distribution of compacted clayey silts. Sci. Eng. Compos. Mater. 22, 623–632.
Vogeler, I., Carrick, S., Cichota, R., Lilburne, R., 2019. Estimation of soil subsurface hydraulic conductivity based on inverse modelling and soil morphology. J. Hydrol. 574, 373–382.
Wagner, J.F., 2013. Mechanical properties of clays and clay minerals. Develop. Clay Sci. 5, 347–381.
Wilson, M.A., et al., 2010. Location and expression of fragic soil properties in a loess-covered landscape, southern Illinois, USA. Geoderma 154, 529–543.
Yates, K., Fenton, C.H., Bell, D.H., 2018. A review of the geotechnical characteristics of loess and loess-derived soils from Canterbury, South Island, New Zealand. Eng. Geol. 236, 11–21.